Radial and axial forces of a passive magnetic bearing

Elkin Rodriguez and Richard Stephan
Universidade Federal do Rio de Janeiro, Rio de Janeiro, BR.
elkinrodvel@msn.com and Richard@dee.ufrj.br

Abstract

Active magnetic bearings require sensors, actuators and controllers, guaranteeing a specified dynamic behavior. Passive Magnetic Bearings, on the other hand, use simpler hardware, but do not have any dynamic control, therefore demanding improvements in the design and optimization process.

This paper presents a contribution to the optimization process and dynamic behavior of PMB with permanent magnets. A single layer and two double layer configurations will be analyzed. Simulation and experimental results of static forces will be compared. Finally, experimental dynamic tests will be carried out.

1 Introduction

The increasing demand for equipment efficiency and longevity has led to the use of magnetic bearings as support devices of moving parts. Active magnetic bearings require sensors, actuators and controllers, guaranteeing a specified dynamic behavior. Passive Magnetic Bearings (PMB), on the other hand, use simpler hardware, but do not have any dynamic control. Their application niche comprises situations of critical power consumption, high reliability and low speed range, for example, wind turbines.

Among the passive magnetic levitation techniques, the configurations using superconductors or permanent magnets are promising. The discovery of superconductor materials, mainly the high critical temperature superconductors (HTS), made applications in energy storage systems of flywheel type [**1**] and MagLev trains [**2**] [**3**] [**4**] industrially interesting.

The use of permanent magnets in PMB was possible due to rare earth magnets. Semi-analytical expressions of the axial force and stiffness have been analyzed, with axial and radial magnetization [**5**] [**6**] [**7**]. The Halbach array and other configurations [**8**] [**9**] can improve the forces. Gyroscopes for satellite and the high-speed compressors are successful applications using PMB with permanent magnets [**10**].

This paper presents a contribution to the optimization process and dynamic behavior of PMB with permanent magnets. A single layer and two double layer configurations will be analyzed. Simulation and experimental results of static forces will be compared. Finally, experimental dynamic tests will be carried out.

2 Ring Magnets

The Passive Magnetic Bearings (PMB) proposed in this paper use two types of ring magnets, that work based on repulsion forces. The geometry of these permanent magnets is shown in Figure 1 and the dimensions are given in Table 1.

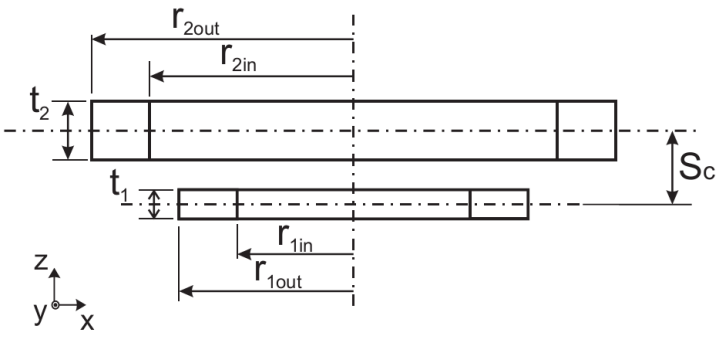

Parameters	Description
r_{1in}	Inner radius of inner ring
r_{1out}	Outer radius of inner ring
t_1	Thickness of inner ring
r_{2in}	Inner radius of outer ring
r_{2out}	Outer radius of outer ring
t_2	Thickness of outer ring
S	Axial distance from geometric center of each magnet

Figure 1. Parameterization of ring magnets used for the construction of the proposed Passive Magnetic Bearings.

TABLE I
DIMENSION OF OUTER AND INNER PERMANENT MAGNETS

Parameters	Length (mm)
r_{2in}	35
r_{2out}	45
t_2	10
R_{1in}	20
r_{1out}	30
t_1	5

3 FEM force calculation

The static forces on passive magnetic bearings were analyzed with the help of the Finite Element Method (FEM) Simulation. The COMSOL software [**11**] was used for these simulation studies.

3.1 Single layer setup

This configuration uses just two permanent magnets; an inner and an outer (Figure 1), with magnetic flux in axial direction. Figure 2 shows the radial and axial force of the magnetic bearing. The radial force shows linearity with the radial displacement (Figure 2a). The increased thickness makes the force larger. The axial force can be considered linear to small displacements (Figure 2b). The thickness affects the location of maximum value of the force. However, displacements higher them 5 mm should take into account the non-linear behavior.

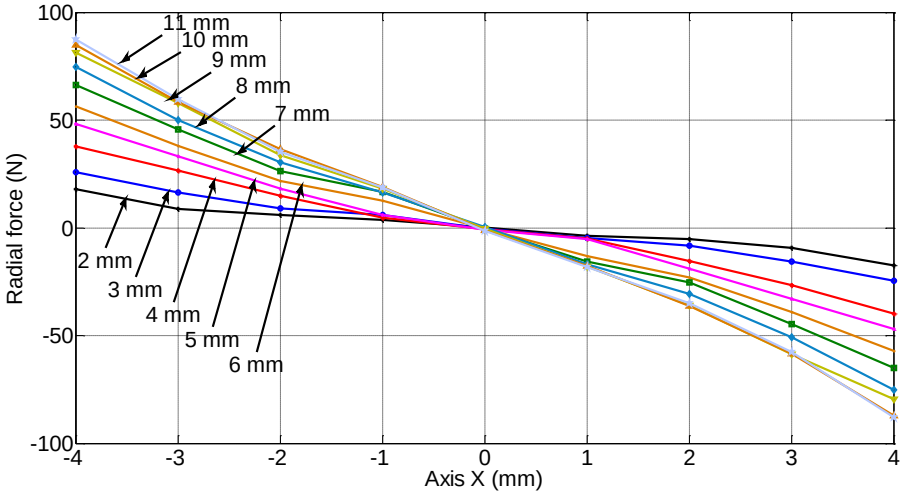

(a)

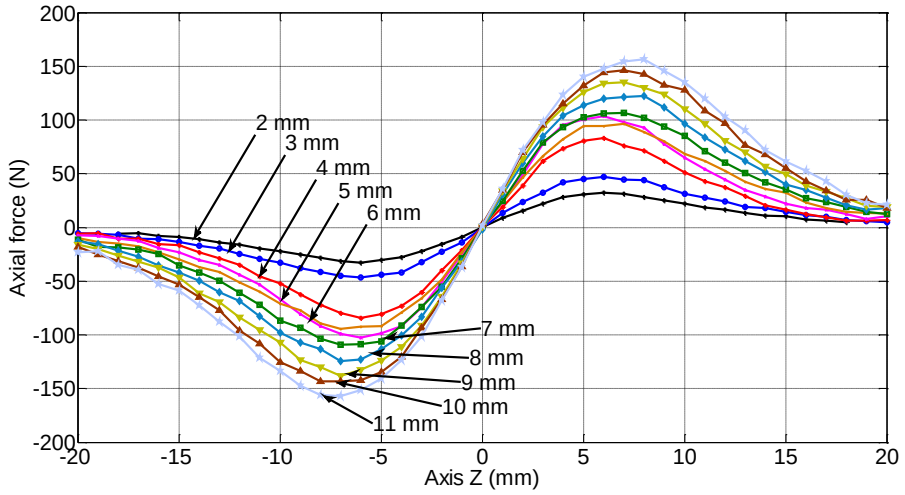

(b)

Figure 2. Behavior of (a) radial and (b) axial forces for different thickness of the inner ring magnet.

3.2 Double layer setup

The double layer setup uses 4 permanent magnets, two outer and two inner (Figure 3). Two configurations will analyze the separation between the outer magnets. Figure 3a shows the outer magnets positioned face to face without separation. The second configuration has a separation S2 of 13 mm between the outer magnets (Figure 3b).

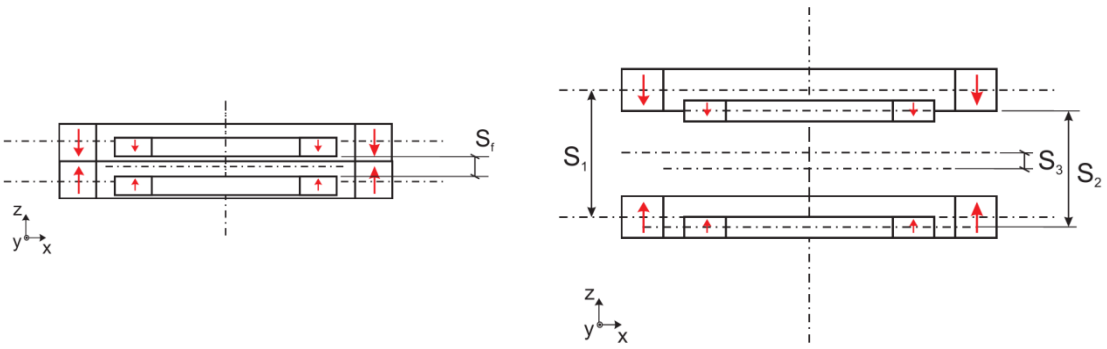

(a) (b)

Figure 3. Passive magnetic bearing for the double layer setup: (a) without separation and (b) with separation.

3.2.1. Without separation of the outer magnets

Figure 4 shows the behavior of the radial and axial forces. This structure has built with a separation of 2.5 mm of the inner magnets, (S_f=2.5 mm in Figure 3a). Radial force has the maximum value of 130 N and it presents a linear response for the radial displacement (Figure 4a). However, the axial displacement provokes a non-linear effect in the radial force.

The axial force (Figure 4b) presents also a non-linear behavior for axial displacements. The maximal axial force occurs with a displacement of approximately 5 mm along the Z axis.

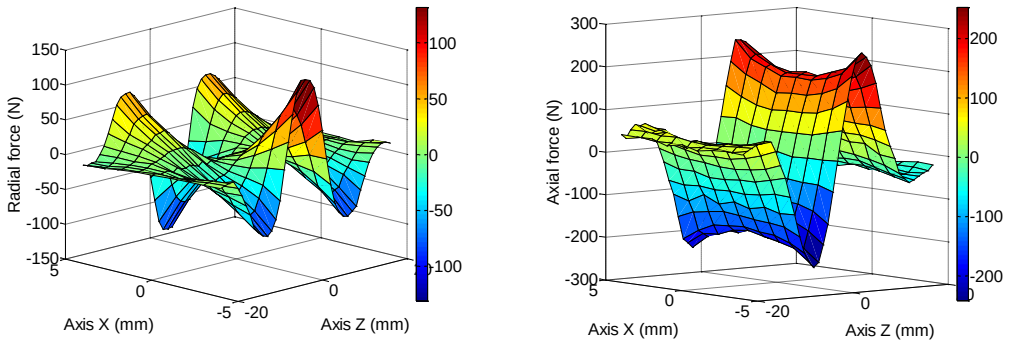

(a) (b)

Figure 4. (a) Radial and (b) axial forces of the double layer setup without separation in the outer magnets.

3.2.2. With separation of the outer magnets

For this structure, the outer and inner magnets holds a separation of 13 and 17 mm between magnets, respectively (Figure 3b). Radial and axial forces are shown in the Figure 5. The maximum value of radial force is 20 N lower than the case without separation. The axial force is 30 N lower.

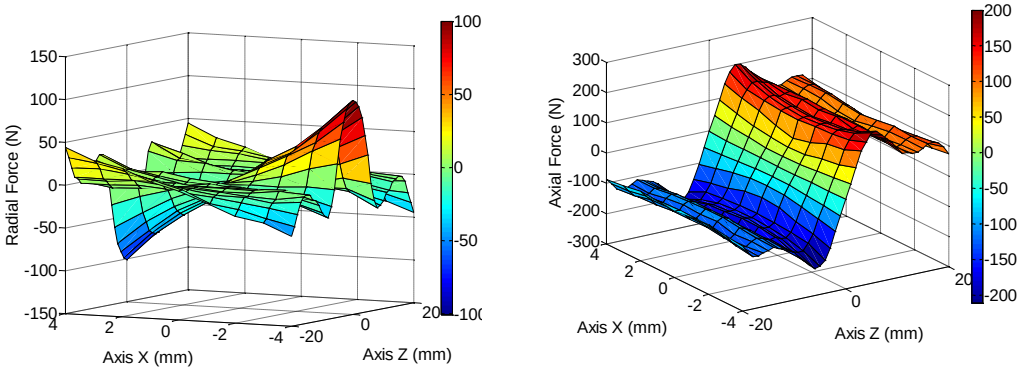

(a) (b)

Figure 5. (a) Radial and (b) axial forces to the double layer setup with separation of the outer magnets (13 mm).

4 Experimental results

4.1 Static test

In order to validate the results derived from simulations, an experimental rig to measure axial and radial forces was built, as shown in Figure 6. This structure can move in two directions, X and Z. The tests require two linear actuators located vertically and horizontally, an ATI load cell [**12**], and the National Instruments PCI-6040e board [**13**].

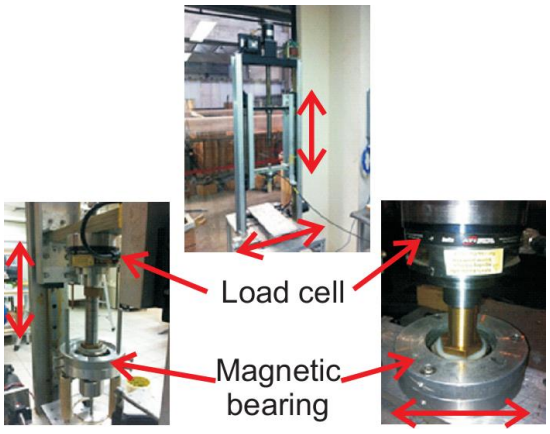

Figure 6. Measurement system

4.1.1. Single layer setup

The comparison of radial and axial forces obtained with FEM simulation and experimental data for the single layer setup are shown in Figure 7. The graphs present similar results, although some FEM simulation data varied mainly due to mesh quality.

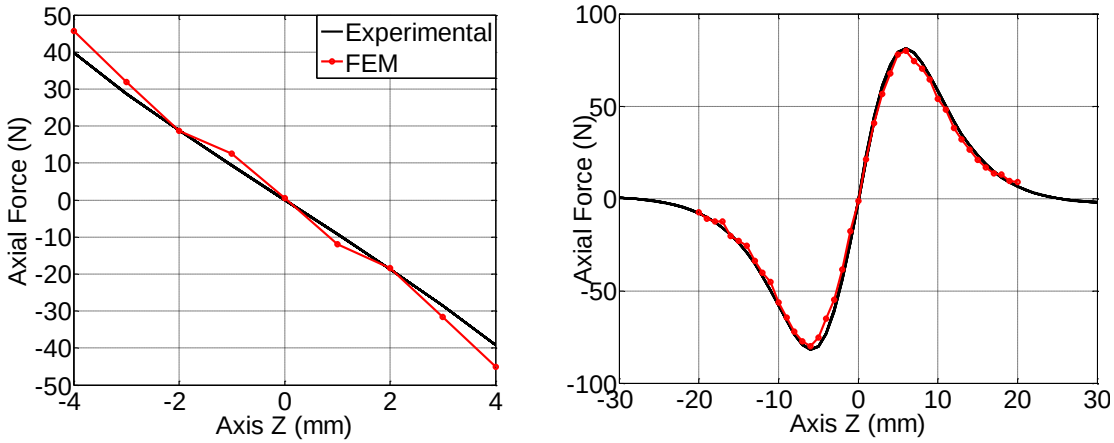

(a) (b)

Figure 7. Comparative of experimental and simulated results (a) radial and (b) axial forces, single layer setup.

4.1.2. Double layer setup

The results of axial and radial forces obtained with FEM are similar in comparison with experimental data for the double layer setup, without and with separation, Figures 8 and 9, respectively. Thus validating the results obtained with the FEM simulation.

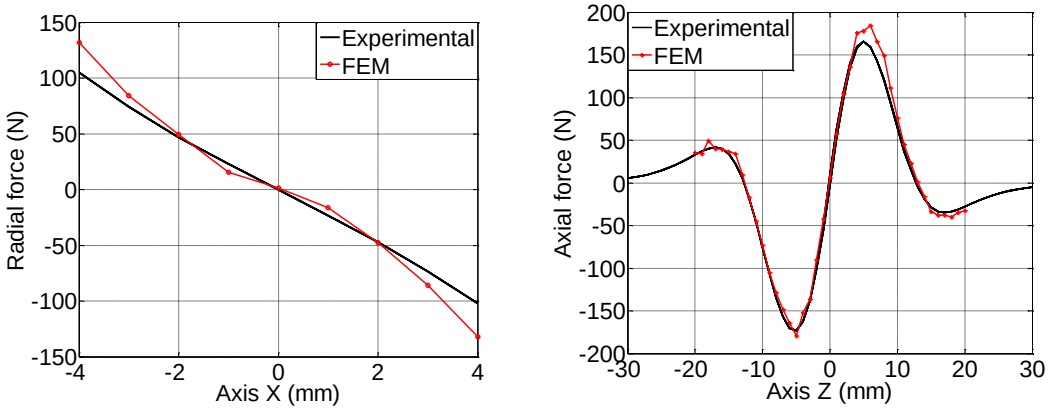

(a) (b)

Figure 8. Comparative of experimental and simulated results (a) radial and (b) axial forces, double layer setup without separation.

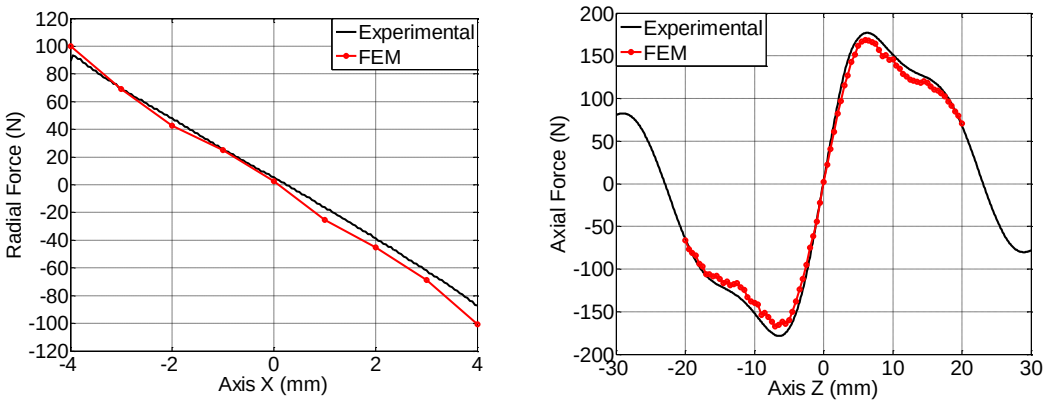

(a) (b)

Figure 9. Comparative of experimental and simulated results (a) radial and (b) axial forces, double layer setup with separation.

4.2 Dynamic tests

A prototype was built to measure the dynamic behavior of the passive magnetic bearing (Figure 10). Forces were measured with the ATI Multi-Axis Force/Torque Delta [**12**] transducer installed at the axis bottom. Eddy current sensors AEC-5210, placed on the base, measure the radial position of the rotor. The velocity was imposed by a motor attached to the prototype by a flexible axis that offers degrees of freedom to the rotor in the connection. The software applied was developed in LabView and the National Instrument board performed the data acquisition.

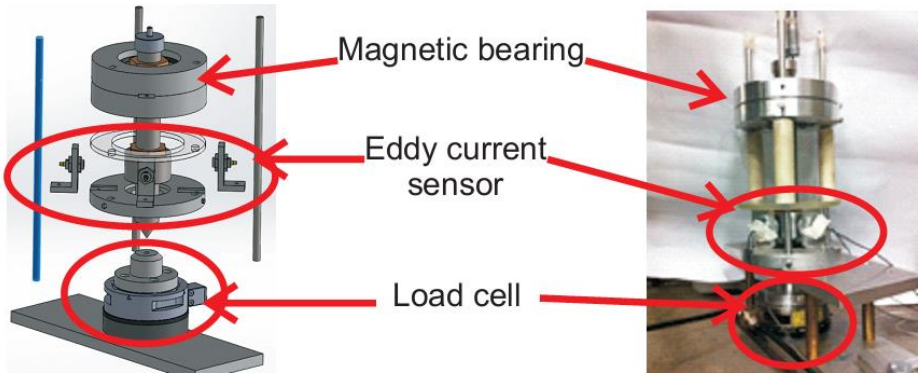

Figure 10. Passive magnetic bearings prototype

4.2.1. Single layer setup

The geometric center of the outer magnet was positioned at 186.2 mm from the pivot point on the load cell. The geometric center of the inner magnet was positioned with help of the load cell, to give an axial force of 20 N. The inner magnet was 2 mm bellow the outer magnet. This can be seen in Figure 7a.

The radial bearings were tested at different speeds. Figure 11 shows a XY graphic, which indicates the behavior of the rotor at 43, 867, 1148, 1370 and 2660 rpm. The average peak to peak displacement and average force in axis Z is shown in Figures 12 and 13, respectively.

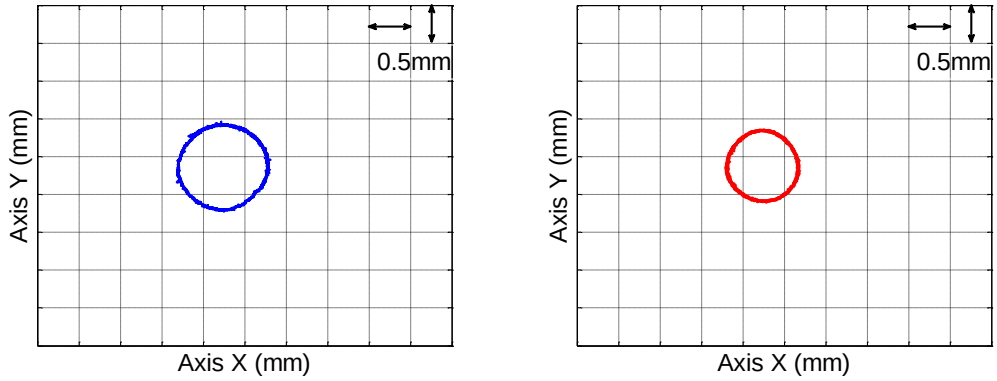

(a) 43 rpm

(b) 867 rpm

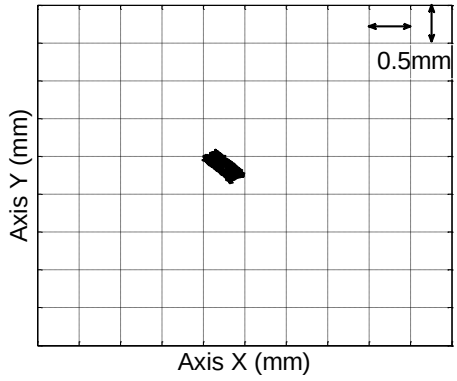

(c) 1148 rpm

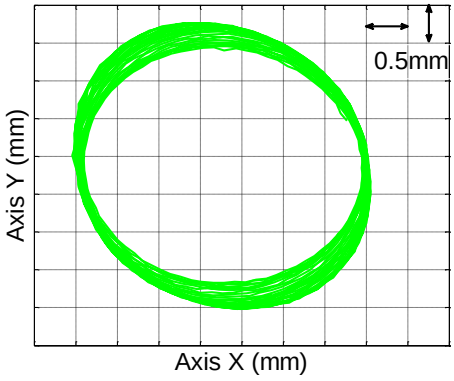

(d) 1370 rpm

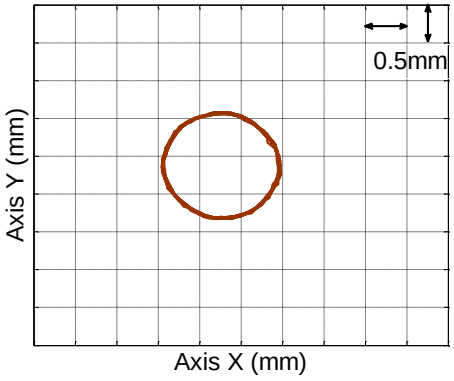

(e) 2660 rpm

Figure 11. Radial orbit of the bearing of single layer setup for 43, 867, 1148, 1370 and 2660 rpm.

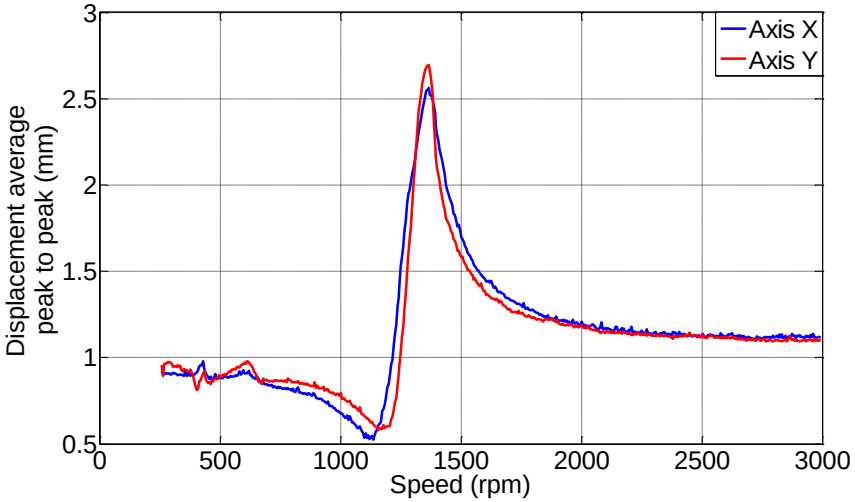

Figure 12. Behavior of rotor position due to velocity changes for the single layer setup.

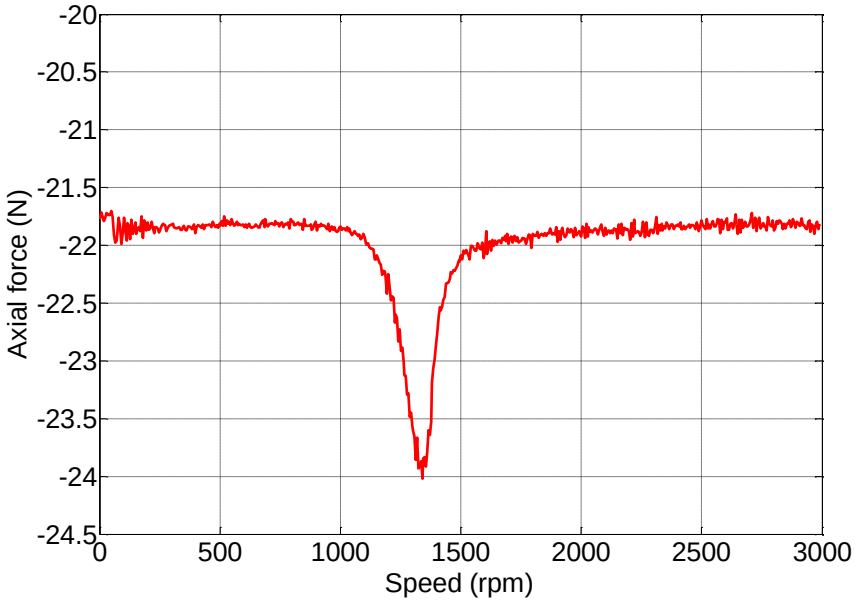

Figure 13. Behavior of the axial force due to velocity changes for the single layer setup.

4.2.2. Double layer setup

The static tests privilege the structure of double layer setup without separation to be selected for the dynamic tests. The geometric center of outer structure was 186.2 mm from the pivot point, equal to single layer setup. The geometric center of inner structure was positioned to give an axial force of 20 N. The centers of outer and inner structures are them 1 mm apart (Figure 8a).

Figure 14 shows the radial orbit of the rotor in XY graphic for 45, 903, 1207, 1740, 2537 and 2919 rpm. The behavior of the rotor position and the axial force are shown in Figures 15 and 16, respectively.

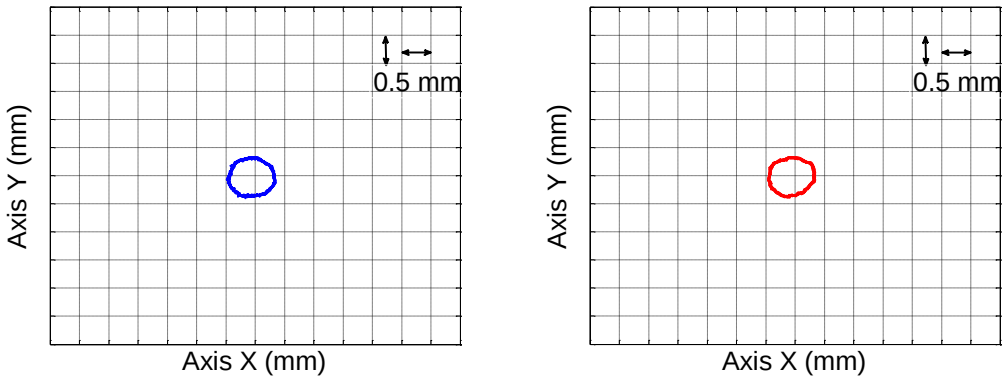

(a) 45 rpm

(b) 903 rpm

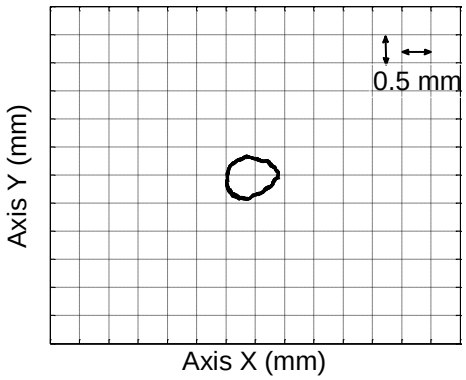

(c) 1207 rpm

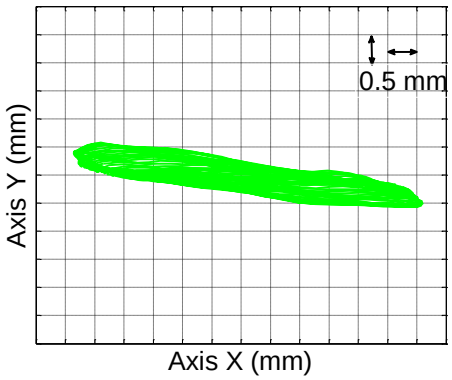

(d) 1740 rpm

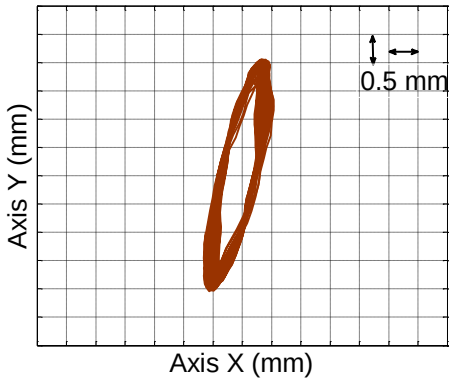

(e) 2537 rpm

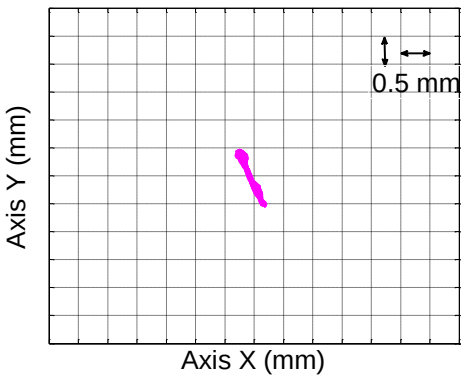

(f) 2919 rpm

Figure 14. Radial orbit of the bearing of double layer setup for 45, 903, 1207, 1740, 2537 and 2919 rpm.

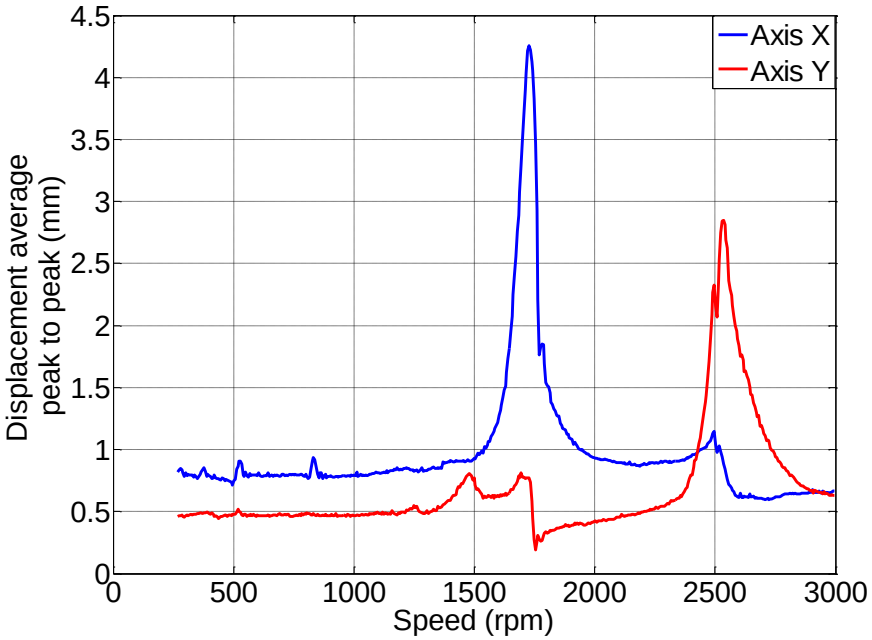

Figure 15. Behavior of rotor position due to velocity changes for the double layer setup.

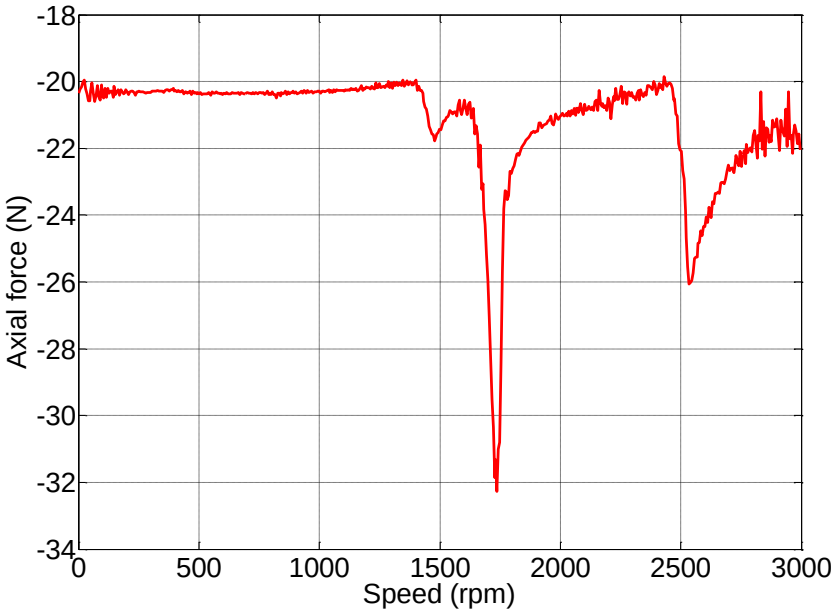

Figure 16. Behavior of the axial force due to velocity changes for the double layer setup.

5 Conclusion

This work presented the static and dynamic performance of two radial passive magnetic bearings arrangements (single layer, double layer). The double layer setup showed a better

behavior, both for static and dynamic tests.

In the two cases, a resonance frequency exists and affects the force intensity, mainly the axial force. The rotor displacement in the single layer setup presents resonance for both axes at the same rotation speed. However, for the double layer setup, the resonance speed is different for each direction, as a consequence of a possible non-homogeneous distribution of magnetic field density in the outer rings magnets. Future studies will examine in greater detail the source of this resonance.

Variations in thickness and radius of the inner magnets affect the magnetic bearing forces. Good agreement between experimental and simulation studies gives confidence on the Finite Element modeling applied. The next step of this research will implement an optimum search algorithm, based on FEM simulation, that will lead to the minimum amount of the magnetic material to produce a desired force, similarly to the work developed for linear bearings [**14**].

6 Acknowledgments

The authors would like to thank the financial support of FAPERJ.

References

[1] G. G. Sotelo, et al., "Halbach array superconducting Magnetic Bearing for a flywheel energy storage system," *IEEE Transactions on Applied Superconductivity*, vol. 15, no. 2, pp. 2253-2256, June 2005.

[2] R. M. Stephan, et al., "Levitation force and stability of superconducting linear bearings using NdFeB and ferrite magnets," vol. 386, pp. 490-494, April 2003.

[3] G. G. Sotelo, et al., "Experimental and Theoretical Levitation Forces in a Superconducting Bearing for a Real-Scale Maglev System," *IEEE Transactions on applied superconductivity*, vol. 21, no. 5, October 2011.

[4] F. N. Werfel, et al., "HTS Magnetic Bearings in prototype application," *IEEE Transactions on applied*, vol. 20, no. 3, p. 1, June 2010.

[5] R. Ravaud, G. Lemarquand and V. Lemarquand, "Force and Stiffness of Passive Magnetic Bearings Using Permanent Magnets. Part 1: Axial Magnetization," *IEEE Transactions on magnetics*, vol. 45, no. 7, pp. 2996-3002, July 2009.

[6] R. Ravaud, G. Lemarquand and V. Lemarquand, "Force and stiffness of passive magnetic bearings using permanent magnets. Part 2: Radial magnetization," *IEEE Transactions on magnetics*, vol. 45, no. 9, pp. 3334-3342, September 2009.

[7] E. P. Furlani, "A formula for the levitation force between magnetic diskc," *IEEE Transactions on magnetics*, vol. 29, no. 6, pp. 4165-4169, November 1993.

[8] Xu Feipeng, Li Tiecai and Lui Yajing, "A study on passive magnetic bearing with Halbach magnetized array," in *International conference on electrical machines and systems, ICEMS-2008*, Wuhan, 2009, pp. 417-420.

[9] Roland Moser, Jan Sandtner and Hannes Bleuler, "Optimization of tepulsive passive magnetic bearings," *IEEE Transactions on magnetics*, vol. 42, no. 8, pp. 2038-2042, August 2006.

[10] Z. Q. Zhu and D. Howe, "Halbach permanent magnet machines and applications: a review," *IEE proceedings electric power applications*, vol. 148, no. 4, pp. 299-308, July 2001.

[11] COMSOL. (2013, May) Introduction to COMSOL Multiphysics. [Online]. HYPERLINK "http://www.comsol.com/shared/downloads/IntroductionToCOMSOLMultiphysics.pdf" http://www.comsol.com/shared/downloads/IntroductionToCOMSOLMultiphysics.pdf

[12] ATI Industrial automation. (2013, February) Compilation of Manuals: F/T Transducer without electronics (TWE) and F/T transducer. http://www.ati-ia.com/app_content/documents/9610-05-1018%20TWE.pdf.

[13] National Instruments. (2013, February) Full-Featured E series multifunction DAQ 12 or 16-Bit, up to 1.25 MS/s, up to 64 analog inputs. http://www.ni.com/pdf/products/us/4daqsc199-201_ETC_212-213.pdf.

[14] E. S. Motta, et al., "Optimization of a linear superconducting levitation system," *IEEE Transactions on applied superconductivity*, vol. 5, no. 21, October 2011.